

Copyright © 1997, by the author(s).
All rights reserved.

Permission to make digital or hard copies of all or part of this work for personal or classroom use is granted without fee provided that copies are not made or distributed for profit or commercial advantage and that copies bear this notice and the full citation on the first page. To copy otherwise, to republish, to post on servers or to redistribute to lists, requires prior specific permission.

VISION-BASED CONTROL OF VEHICLES

by

J. Košecká, R. Blasi, C. J. Taylor, and J. Malik

Memorandum No. UCB/ERL M97/67

10 August 1997

COVER PAGE

VISION-BASED CONTROL OF VEHICLES

by

J. Košecká, R. Blasi, C. J. Taylor, and J. Malik

Memorandum No. UCB/ERL M97/67

10 August 1997

ELECTRONICS RESEARCH LABORATORY

College of Engineering
University of California, Berkeley
94720

Vision-Based Control of Vehicles

J. Košecká, R. Blasi, C. J. Taylor and J. Malik

Department of Electrical Engineering and Computer Sciences

University of California at Berkeley

Berkeley, CA 947

Abstract

We describe the problem of automated steering using computer vision, focusing on an analysis of the problem and the design of appropriate controller. Realistic assumptions about the quality and availability of the measurements extracted from image sequences are taken into account. We investigate various static feedback strategies where the measurements obtained from vision, namely offset from the centerline and angle between the road tangent and the orientation of the vehicle at some look-ahead distance, are directly used for control. Within this setting we explore the role of look-ahead, its relation to the vision processing delay, longitudinal velocity and road geometry. Results from ongoing experiments with our autonomous vehicle system are presented along with simulation results.

1 Introduction and Motivation

This paper addresses the problem of designing control systems for steering a motor vehicle along a highway using the output from a video camera mounted inside the vehicle. Several aspects of this problem have been examined extensively in the past, both in the psychophysics literature as well as in control theoretic studies. Land and his colleagues [LL94] studied the correlation between the direction of gaze and the steering performance of human drivers. They assert that drivers make use of perceptually salient tangent points on the images of the lane markers to negotiate curves in the road. The preview information that the drivers obtain from vision has been shown to be sufficient for driving tasks even in the presence of a substantial delay between gaze-shift to the next tangent point and steering movements. Part of the delay was attributed to time it takes to process visual information [Lan96].

Land and Horwood showed that human drivers make use of information from various look-ahead ranges in front of the vehicle. They suggest that drivers use the information from the further regions of the roadway for anticipatory control while the information about the roadway in the near look-ahead region is primarily used to regulate the lateral position of the vehicle within the lane.

Control theoretic studies have been done for both kinematic and dynamic models of vehicles. In the kinematic setting there have been several attempts to formulate the vision based steering task in the image plane. Authors in [RH91] suggested the use of measurement of the projection of the road's tangent point

and its optical flow in the image for generating steering commands. The steering rate control commands were made proportional to the flow of the tangent point and the angle of the tangent line with respect to the car. The stability and sensitivity issues of this approach have not been explored.

The automated steering task has also been formulated within the visual servoing paradigm. A stability analysis was provided for an omnidirectional mobile base trying to align itself with a straight road [ECR92] or nonholonomic mobile base following an arbitrary ground analytic curve [MKS97].

The controllers designed based on kinematic models were either tested in simulations or the experiments were performed at speeds below 20 m/s. However at higher speeds dynamic effects are quite pertinent and the need for a dynamic model becomes apparent.

The control problem in a dynamic setting, using measurements ahead of the vehicle, has been explored by [ÖÜH95] who proposed a constant control law proportional to the offset from the centerline at a look-ahead distance. Their analysis showed that closed loop stability for this controller can always be obtained by increasing the look-ahead distance to an appropriate value. In their experiments the look-ahead distance was chosen to be proportional to the longitudinal velocity of the vehicle. This analysis holds for a general class of look-ahead systems, where the measurements are naturally available ahead of the car (e.g. radar, vision); however, it did not take into account the effects of delay (in case of visual processing) on the overall performance of the system.

Dickmanns, et al [DM92] successfully demonstrated a vision-based autonomous steering system in 1985. They developed a Kalman-filter based observer which estimated the position and orientation of the vehicle with respect to the road along with the road geometry. The state estimates provided by the observer were then used for full state feedback using a pole-placement method. The estimate of the curvature of the road was used in a feedforward control law and improved the road following behavior of the system.

Another class of references involves both theoretical and experimental studies of the steering problem. The studies typically use a small and fixed look-ahead distance and the control objective is formulated either at the look-ahead distance [GTP96] or at the center of gravity of the vehicle [Pen92]. An analysis of the tradeoffs between the performance requirements and robustness of the overall system can be found in [GTP96]. Various control laws have been proposed, compensating for the small look-ahead distance, while still achieving desired performance.

This paper will discuss the problem of automated steering using computer vision, focusing on the analysis of the problem and controller design choice. Realistic assumptions about the quality and availability of the measurements extracted from image sequences are taken into account. We investigate various static feedback strategies where the measurements obtained from vision, namely offset from the centerline and angle between the road tangent and the orientation of the vehicle at some look-ahead distance, are directly used for control. Within this setting we explore the role of look-ahead, its relation to the vision processing delay, longitudinal velocity and road geometry.

2 Modeling

The dynamic behavior of the vehicle can be described by a detailed 6-DOF nonlinear model [Pen92]. Since it is possible to decouple the longitudinal and lateral dynamics, a linearized model of the lateral vehicle dynamics is used for controller design. The linearized model of the vehicle retains only lateral and yaw dynamics, assumes small steering angles and a linear tire model, and is parameterized by the current longitudinal velocity. Lumping the two front wheels and two rear wheels together, the resulting “bicycle model” (Figure 2) is described by the following variables and parameters (Table 1):

v linear velocity vector with two components (v_x, v_y) , where v_x denotes speed

α_f, α_r side slip angles of the front and rear tires respectively

ψ vehicle yaw angle with respect to a fixed inertial frame

δ_f front wheel steering angle

δ commanded steering angle

m total mass of the vehicle

I_ψ total inertia of the vehicle around center of gravity (CG)

l_f, l_r distance of the front and rear axles from the CG

l distance between the front and the rear axle $l_f + l_r$

c_f, c_r cornering stiffness of the front and rear tires.

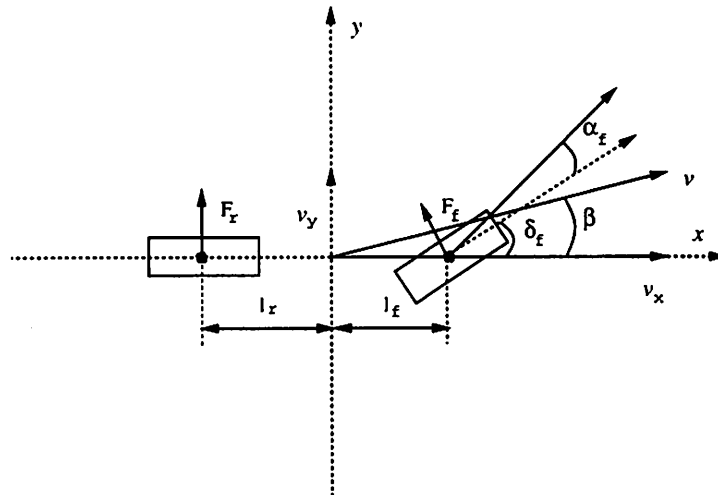


Figure 1: The motion of the vehicle is characterized by its velocity $v = (v_x, v_y)$ expressed in the vehicles inertial frame of reference and its yaw rate $\dot{\psi}$. The forces acting on the front and rear wheels are F_f and F_r , respectively. The side slip angles α_f, α_r denote the differences between the current steering angles and the velocity vectors of the front and rear wheels respectively. The steering angle of the front wheel is δ_f , the distance of the axles to the center of gravity of the vehicle are l_f and l_r .

The lateral dynamics equations are obtained by computing the net lateral force and torque acting on the vehicle following Newton-Euler equations [Kos97] and choosing $\dot{\psi}$ and v_y , as state variables. The state

m	I_ψ	l_f	l_r	$c_f = c_r$
1590 kg	2920 kg m ²	1.22 m	1.62 m	2×60000 N/rad

Table 1: Parameters for a Honda Accord. The cornering stiffness is increased by factor 2 since the two tires are lumped together.

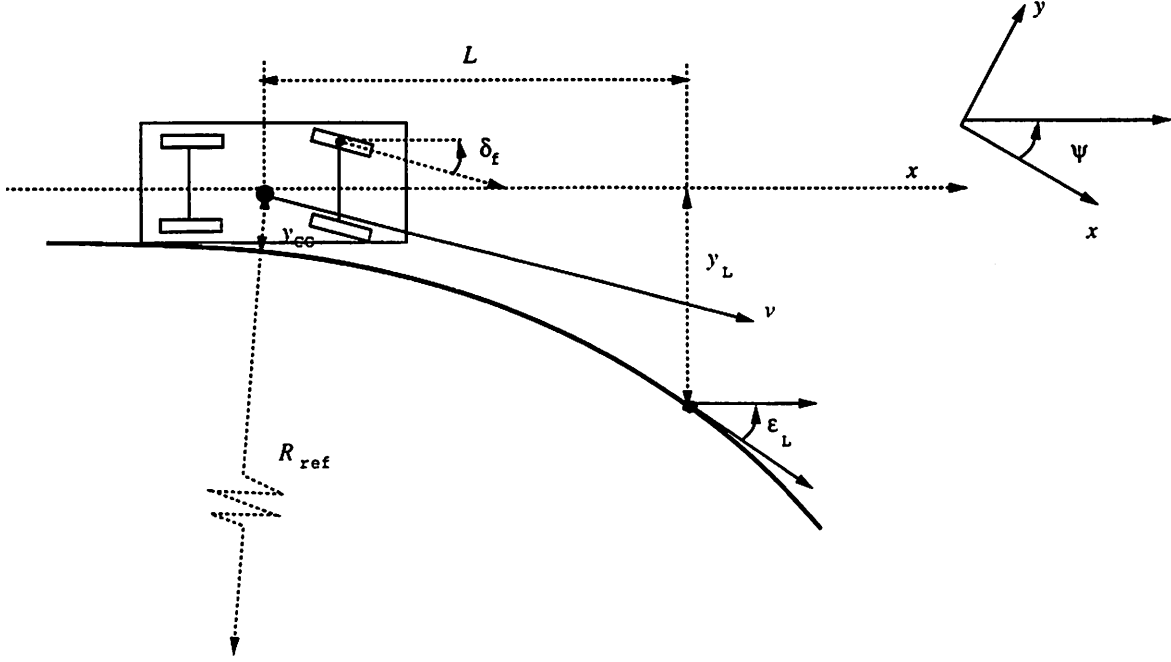


Figure 2: The vision system estimates the offset from the centerline y_L and the angle between the road tangent and heading of the vehicle ϵ_L at some look-ahead distance L .

equations have the following form:

$$\begin{bmatrix} \dot{v}_y \\ \ddot{\psi} \end{bmatrix} = \begin{bmatrix} -\frac{c_f+c_r}{mv_x} & -v_x + \frac{c_r l_r - c_f l_f}{mv_x} \\ \frac{-l_f c_f + l_r c_r}{I_\psi v_x} & -\frac{l_f^2 c_f + l_r^2 c_r}{I_\psi v_x} \end{bmatrix} \begin{bmatrix} v_y \\ \dot{\psi} \end{bmatrix} + \begin{bmatrix} \frac{c_f}{m} \\ \frac{l_f c_f}{I_\psi} \end{bmatrix} \delta_f \quad (1)$$

2.1 Vision Dynamics

The additional measurements provided by the vision system (see Figure 2) are:

y_L the offset from the centerline at the look-ahead distance,

ϵ_L the angle between the tangent to the road and the vehicle orientation

L the look-ahead distance at which these measurements are taken.

K_L the curvature of the road at the look-ahead distance,

The equations capturing the evolution of these measurements due to the motion of the car and changes

in the road geometry are:

$$\dot{y}_L = v \varepsilon_L - v_y - \dot{\psi} L \quad (2)$$

$$\dot{\varepsilon}_L = v K_L - \dot{\psi} \quad (3)$$

The rate of the change \dot{y}_L of the offset at the look-ahead distance is proportional to the velocity v and the current angle between the vehicle orientation and the road tangent ε_L , lateral velocity v_y , and yaw rate of the car $\dot{\psi}$ scaled by the look-ahead distance L . The second equation expresses the fact that the rate of change of the angle between the road and the car at the look-ahead distance $\dot{\varepsilon}_L$ is proportional to the velocity v scaled by the curvature at the look-ahead K_L and the yaw rate of the vehicle $\dot{\psi}$.

Combining the vehicle lateral dynamics with the vision dynamics into a single dynamical system of the form:

$$\dot{\mathbf{x}} = \mathbf{A} \mathbf{x} + \mathbf{B} \mathbf{u} + \mathbf{E} \mathbf{w}$$

$$\mathbf{y} = \mathbf{C} \mathbf{x} + \mathbf{D} \mathbf{u} + \mathbf{F} \mathbf{w}$$

with the state $\mathbf{x} = [v_y, \dot{\psi}, y_L, \varepsilon_L]^T$ and control input $\mathbf{u} = \delta_f$ and disturbance $\mathbf{w} = K_L$ leads to the following state equations:

$$\begin{bmatrix} \dot{v}_y \\ \ddot{\psi} \\ \dot{y}_L \\ \dot{\varepsilon}_L \end{bmatrix} = \begin{bmatrix} -\frac{c_f+c_r}{mv_x} & -v_x + \frac{c_r l_r - c_f l_f}{mv_x} & 0 & 0 \\ \frac{-l_f c_f + l_r c_r}{I_\psi v_x} & -\frac{l_f^2 c_f + l_r^2 c_r}{I_\psi v_x} & 0 & 0 \\ -1 & -L & 0 & v_x \\ 0 & -1 & 0 & 0 \end{bmatrix} \begin{bmatrix} v_y \\ \dot{\psi} \\ y_L \\ \varepsilon_L \end{bmatrix} + \begin{bmatrix} \frac{c_f}{m} \\ \frac{l_f c_f}{I_\psi} \\ 0 \\ 0 \end{bmatrix} \delta_f + \begin{bmatrix} 0 \\ 0 \\ 0 \\ v_x \end{bmatrix} K_L \quad (4)$$

The output equations have following form:

$$\mathbf{y} = \begin{bmatrix} -\frac{c_f+c_r}{mv_x} & \frac{c_r l_r - c_f l_f}{mv_x} & 0 & 0 \\ 0 & 1 & 0 & 0 \\ 0 & 0 & 1 & 0 \\ 0 & 0 & 0 & 1 \end{bmatrix} \begin{bmatrix} v_y \\ \dot{\psi} \\ y_L \\ \varepsilon_L \end{bmatrix} + \begin{bmatrix} \frac{c_f}{m} \\ 0 \\ 0 \\ 0 \end{bmatrix} \delta_f \quad (5)$$

The road curvature K_L enters the model as an exogenous disturbance signal.

3 Vision System

The vision-based lane tracking system used in our experiments is an improved version of the one presented at last year's ITS conference [TMW96]. This system takes its input from a single forward-looking CCD

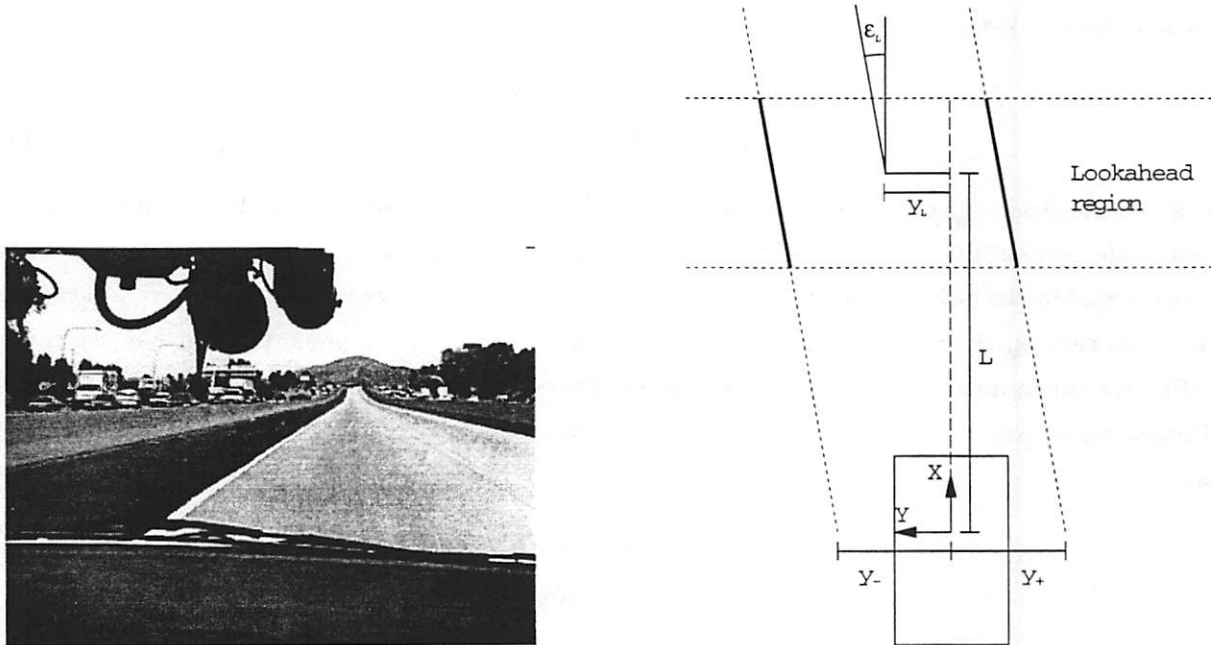


Figure 3: (Left) The camera setup. (Right) The position of the vehicle with respect to the lane.

video camera. It extracts potential lane markers from the input using a simple template-based scheme. It then finds the best linear fits to the left and right lane markers over a certain look-ahead range through a variant of the Hough transform. This robust fitting strategy allows us to overcome spurious lane markings and other distracting features that are common on California's highways.

From the measurements of the positions of the left and right lane markers in the video images we can compute an estimate for the lateral position and orientation of the vehicle with respect to the roadway at a particular look-ahead distance, L , as shown in Figure 3. The vision system is implemented on an array of TMS320C40 digital signal processors which are hosted on the bus of an Intel-based industrial computer. The system processes images from the video camera at a rate of 30 frames per second. The total delay between the time the shutter on the CCD video camera is closed and the time the results for that image are available to the control computer is 57 milliseconds. Since the delay is quite substantial we will explicitly consider it in the controller design.

4 Analysis

The aim of this analysis is to understand the relationship between the steering command and the output of the vision system y_L at various velocities and various road conditions as well as the road tracking capability of the car under various road geometries. The vision-based lateral steering system is composed of three subsystems:

- **Action:** The car dynamics characterized by a transfer function between steering angle δ_f and lateral and yaw accelerations at the center of gravity of the vehicle ¹.
- **Perception:** The vision subsystem which provides positional measurements of the offset from the centerline at the look-ahead and the angle with respect to the road. The offset at the look-ahead is affected by the curvature of the road.
- **Environment:** In this case, represented by the curvature of the road which is modeled as an external disturbance signal.

The block diagram of the overall system following the state equations is in Figure 4. The transfer function $V_1(s)$ between the steering angle δ_f and offset at the look-ahead y_L and $V_2(s)$ between δ_f and ϵ_L can be obtained by taking a Laplace transform of the state equations. The transfer functions $V_1(s)$ and $V_2(s)$ share a denominator $P(s)$:

$$P(s) = s^2(s^2 v_x^2 m I_\psi + s v_x (I_\psi (c_f + c_r) + m(c_f l_f^2 + c_r l_r^2)) + c_f c_r l^2 + m v_x^2 (c_f l_f + c_r l_r)) \quad (6)$$

and have the following form:

$$V_1(s) = \frac{s^2 v_x^2 c_f I_\psi + s v_x c_r c_f (l_f l_r + l_r^2) + c_r c_f v_x^2 l + L(s^2 v_x^2 c_f l_f m + s v_x c_r c_f l)}{P(s)} \quad (7)$$

$$V_2(s) = \frac{s^2 c_f l_f m v_x^2 + s c_f c_r v_x l}{P(s)} \quad (8)$$

From (7) and (8) we observe that the lateral offset at the look-ahead y_L can be written as a sum of the lateral offset at the center of the gravity and the yaw at the center of the gravity scaled by look-ahead distance L :

$$V_1(s) = V(s) + L V_2(s) \quad (9)$$

where $V(s)$ is the transfer function between the offset at the center of the gravity y_{CG} and δ_f . Equation (9) can be rewritten by singling out the vehicle dynamics in terms of \ddot{y}_{CG} and $\ddot{\psi}$ followed by the integrating action $1/s^2$:

$$V_1(s) = \frac{1}{s^2} (G(s) + L G_2(s)) \quad (10)$$

There are two additional components which appear in the block diagram. The actuator $A(s)$ is modeled as a low pass filter of the commanded steering angle δ . The actual steering angle of the front wheel δ_f is then

$$\delta_f(s) = A(s)\delta(s). \quad (11)$$

The second component is a pure time delay element $e^{-T_d s}$ representing the latency T_d of the vision subsystem. The exponential function can be approximated by a rational function using the Padé approximation [FPEN94] and becomes:

$$D(s) = e^{-T_d s} \approx \frac{2 - T_d s}{2 + T_d s} \quad (12)$$

In our system $T_d = 0.057$ s. The transfer function $C(s)$ corresponds to the controller to be designed.

¹An additional component of the action subsystem is the actuator, which often imposes some practical constraints on the design of the control strategy. We omitted the actuator model while studying conceptual issues

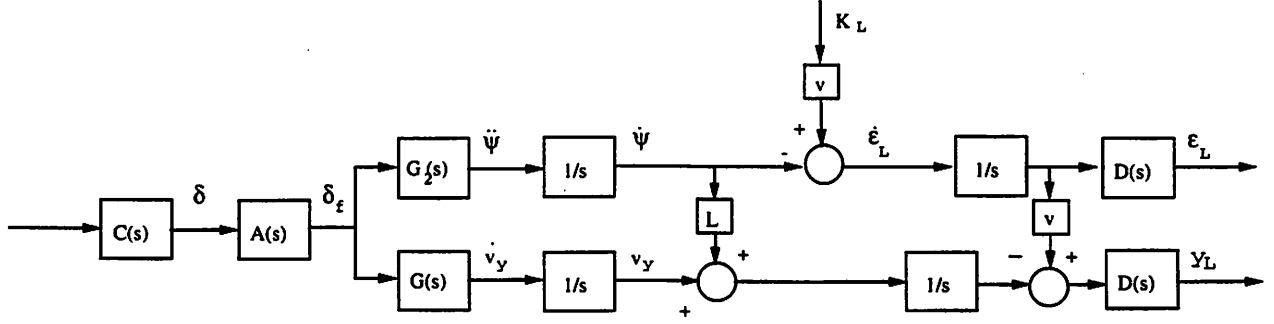


Figure 4: The block diagram of the overall system with the two outputs provided by the vision system.

4.1 Control objective

The vehicle control objective is to follow the reference path specified by radius R_{ref} (curvature $K_{ref} = \frac{1}{R_{ref}}$). Perfect tracking of the road (Figure 5) in steady state corresponds to the zero offset $y_{CG} = 0$ of the vehicle's center of the gravity from the centerline, with the orientation of the vehicle aligned with the tangent to the road. Fixing the look-ahead distance, at steady state we have: $\dot{\epsilon}_L = 0$, $\dot{y}_L = 0$, $\dot{v}_y = 0$, $\ddot{\psi} = 0$ and v_{yref} , ψ_{ref} and δ_{ref} . In such case the yaw rate $\dot{\psi}_{ref}$ can be obtained from (3) as reference signal:

$$\dot{\psi}_{ref} = K_{ref} v. \quad (13)$$

The control objective can be also formulated at the lateral acceleration level, where the goal is to match the lateral acceleration at the center of the gravity with the reference lateral acceleration:

$$\ddot{y}_{ref} = K_{ref} v^2.$$

The latter formulation allows us to put bounds on lateral acceleration and adjust longitudinal velocity accordingly while following a curve of a given curvature K_{ref} . Lateral acceleration of 0.3-0.4g, where $g = 9.81 \text{ m/s}^2$, has been shown to be comfortably accepted by humans. In addition to limits on the steady-state lateral acceleration an important design criterion is that of passenger comfort. This is typically expressed in terms of jerk, corresponding to the rate of change of acceleration. For a comfortable ride no frequency above 0.1 - 0.5 Hz should be amplified in the path to lateral acceleration [GTP96]. This frequency range places limit on the bandwidth of the closed-loop transfer function of the system. This limit also reduces susceptibility of the system to sensor noise.

While the passenger comfort criteria are imposed on the path between steering angle δ_f and lateral acceleration \ddot{y}_L , the road following performance criteria are captured by the transfer function $F(s) = \frac{y_L(s)}{K_{ref}(s)}$, between reference lateral acceleration $\ddot{y}_{ref} (K_{ref} v^2)$ and y_L :

$$F(s) = \frac{v^2}{s^2 + C(s) A(s) V_1(s) D(s)}. \quad (14)$$

The road following criteria can be specified in terms of maximal allowable offset y_{Lmax} as a response to the step change in curvature as well as bandwidth requirements on the transfer function $F(s)$ [GTP96].

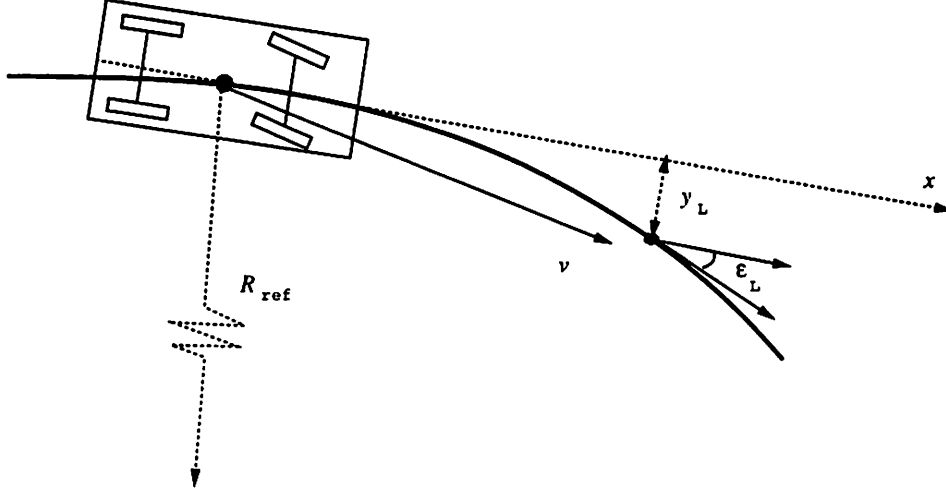


Figure 5: Perfect tracking of the road with reference radius R_{ref} .

In the remainder of this section we will concentrate primarily on the stability issues and controller design which satisfies the criteria for passenger comfort. Since the primary advantage of the vision system is the availability of measurements at a point ahead of the vehicle, we will analyze how the choice of the look-ahead distance L affects the transfer function $V_1(s)$ between steering angle and the offset at the look-ahead. The analysis will also take into account the processing delay T_d inherent in the vision system which substantially affects the stability of the system.

Look-ahead and Delay A root locus of the transfer function $V_1(s)$ is in Figure 6. The transfer function $V_1(s)$ has four poles and two zeros, where the damping of the zero pair affects the location of closed loop poles and subsequently the transient response of the system more profoundly. Figure 6a depicts the effect of increasing the look-ahead on the damping of the zero pair at $v_x = 20$ m/s and look-ahead $L = 2, 5, 7, 10$ m. As the look-ahead increases the zeros move closer to the real axis, improving the damping of the closed loop poles of $V_1(s)$. Increasing the velocity moves both poles and zeros of $V_1(s)$ towards the imaginary axis, resulting in a poor damping of the poles. The root locus of transfer function $V_1(s)$ for different velocities $v_x = 10, 15, 20, 30$ m/s is in Figure 6b. The choice of proper look-ahead distance is therefore crucial for stability and performance of the system. Increasing the look-ahead improves the damping of the closed loop poles of $V_1(s)$.

Another parameter which affects the behavior of the overall system is the delay associated with the vision system. The effect of the delay can be more conveniently examined in the frequency domain in terms of Bode plots. The delay element adds an additional phase lag over the whole range of frequencies having a clear

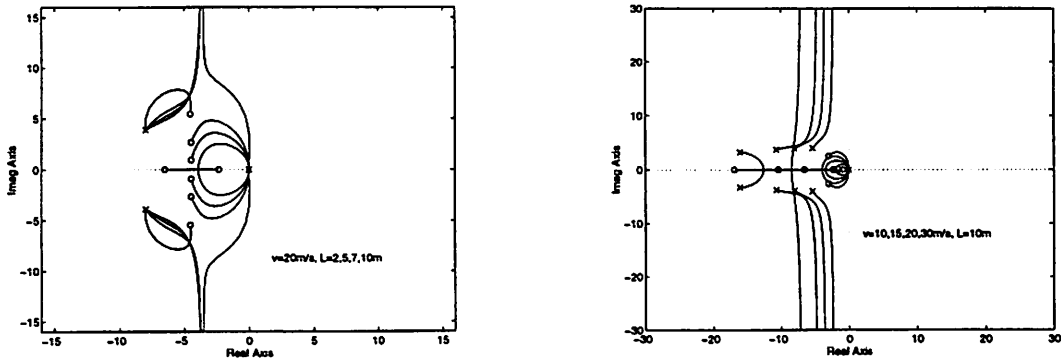


Figure 6: (a) Increasing the look-ahead distance L moves the zeros of the transfer function $V_1(s)$ closer to the real axis, which improves their damping. Once they reach the real axis, further increasing of the look-ahead doesn't have any effect on damping. The poles of the transfer function are not affected by changes in L since the parameter appears only in the numerator of $V_1(s)$. (b) Root locus of $V_1(s)$ for velocities $v_x = 10, 15, 20, 30$ m/s and fixed look-ahead distance $L = 10$ m. Increasing the velocity v_x moves both the poles and zeros towards the imaginary axis.

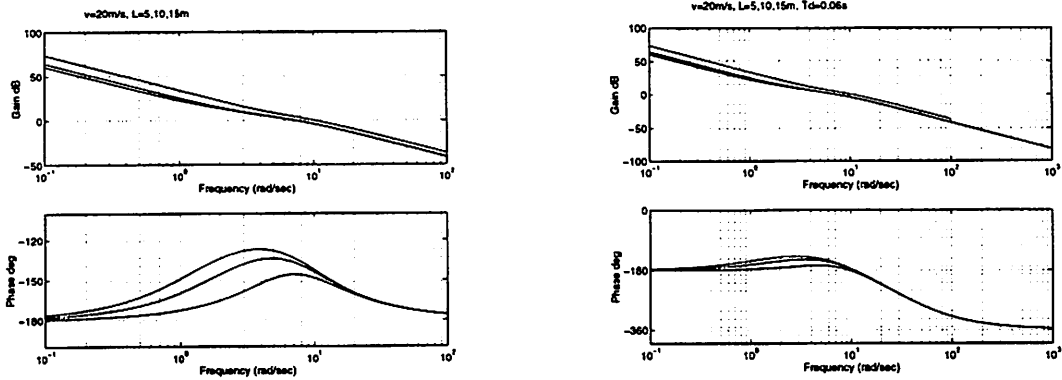


Figure 7: (a) Bode plot $V_1(s)$ for varying look-ahead $L = 5, 10, 15$ m at $v_x = 20$ m/s with no delay. Increasing the look-ahead adds substantial phase lead at the crossover frequency. (b) Bode plot of $V_1(s)D(s)$. The presence of the delay adds an additional phase lag over the whole range of frequencies. The look-ahead of 15 m at $v_x = 20$ m/s provides 38.07° phase margin, with appropriate gain adjustment of $K=0.05$. When the look-ahead decreases or speed increases the phase margin in the presence of delay diminishes and the system becomes unstable. Choosing larger look-ahead is more crucial in the presence of delay.

destabilizing effect on the overall system and limiting system's bandwidth. Ideally the system should have infinite gain margin and about 40-60° phase margin at the crossover frequency. Bode diagrams of $V_1(s)$ and $V_1(s) D(s)$ in Figure 7 demonstrate the interplay between look-ahead and delay. The crossover frequency has been shifted by a gain factor to the region where the maximum phase lead occurs. For smaller speeds the delay in our system can be compensated by additional phase lead provided by increased look-ahead distance and by adjusting the proportional gain of the system, for higher speeds proportional compensation is not sufficient and additional lead action is necessary in order to achieve sufficient phase margin at the crossover frequency of 0.1 - 0.5 Hz in order satisfy criteria for passenger comfort.

4.2 Controller Design

The analysis in the previous section demonstrated that at velocities up to 15 m/s the look-ahead can guarantee satisfactory damping of the closed loop poles of $V_1(s)$ and compensate for the delay using simple unity feedback control with proportional gain in the forward loop. As the velocity increases the transient response is affected more by poor damping of the poles of $V_1(s)$ introducing additional phase lag around the 0.1 - 2 Hz. Since further increasing the look-ahead does not improve the damping, gain compensation only cannot achieve satisfactory performance (see Figure 8).

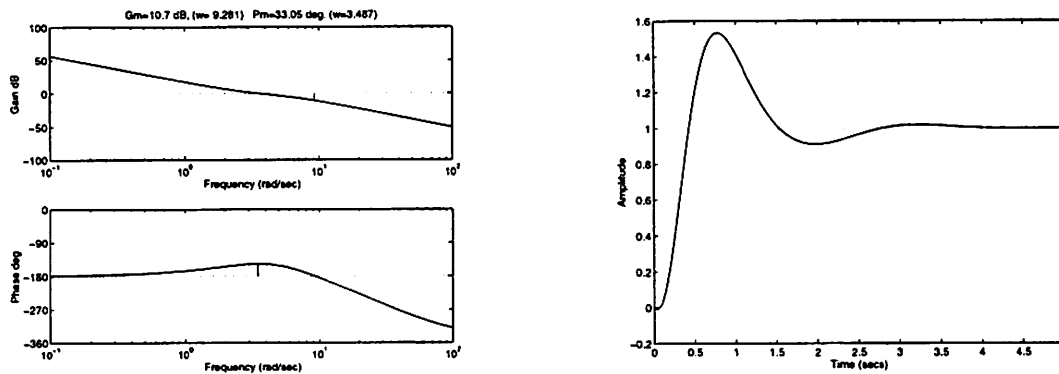


Figure 8: Gain compensation: maximum phase lead which is achievable at $v_x = 30$ m/s, $T_d = 0.06$ s by the means of gain compensation and increasing the look-ahead up to 15 m is 33°-not sufficient for satisfactory damping.

Looking at the bode plot of the open loop transfer function $V_1(s)$ in Figure 8 natural choice for obtaining an additional phase lead in the frequency range 0.1 - 2 Hz would be to introduce some derivative action. This can be done by a PD controller. However pure derivative action has an effect of increasing the bandwidth of the system which is undesirable for passenger comfort. In order to keep the the bandwidth low an additional lag term is necessary.

One possible lead-lag controller has the following form:

$$C(s) = K \frac{T_1 s + 1}{(\alpha T_1 s + 1)(T_2 s + 1)} = \frac{0.09s + 0.18}{0.025s^2 + 1.5s + 20} \quad (15)$$

where $C(s)$ is a lead network in series with a single pole. The above controller was designed for a velocity of 30 m/s (108 km/h, 65 mph), a look-ahead of 15 m and 60 ms delay. It also takes into account the limited

bandwidth of the actuator, which was modeled via standard system identification techniques. The resulting closed loop system has a bandwidth 0.45 Hz with a phase lead of 45° at the crossover frequency. Discretized version of the above controller taking into account 30 ms sampling time of the control loop becomes:

$$u_k = 0.7u_{k-1} - 0.1u_{k-2} + 0.85y_{Lk} + 0.054y_{Lk-1} - 0.79y_{Lk-2}$$

where u_k is the commanded steering angle at time k and y_{Lk} is the measurement of the offset at the look-ahead at time k .

Since increasing the speed has a destabilizing effect on $V_1(s)$, designing the controller for the highest intended speed automatically guarantees stability at lower speeds and achieves satisfactory ride quality. In order to tighten the tracking performance at lower speeds individual controllers can be designed for various speed ranges and gain scheduling techniques used to interpolate between them. An alternative adaptive self-tuning control scheme such as Ziegler-Nichols tuning rules could also be used [Bla97].

We can conclude that sufficiently large look-ahead affects favorably both the stability and performance of the system and can partially compensate for the delay present in the sensory system. For higher velocities an additional derivative action is necessary in order to provide satisfactory phase margin. An alternative would be to further increase look-ahead to obtain the needed phase lead. However this is undesirable since the accuracy of the measurements from the vision system decreases as the look-ahead increases and is also affected by the speed of the vehicle. Furthermore large look-ahead distances also affect negatively the transient behavior of the vehicle when it encounters large changes in the road curvature. This transient behavior of the controller can be further improved by a feedforward control component. The steady state behavior of the system during perfect tracking of a curve with radius R_{ref} , is characterized by particular values of $\dot{\psi}_{ref}$, v_{yref} and δ_{ref} . By setting the $[\dot{v}_y, \ddot{\psi}, \dot{y}_L, \dot{\epsilon}_L]^T$ to 0, the steering angle δ_{ref} can be obtained from state equations after some algebraic manipulation and becomes:

$$\delta_{ref} = K_{ref} \left(l - \frac{(l_f c_f - l_r c_r) v_x^2 m}{c_r c_f l} \right). \quad (16)$$

The feedforward control law essentially provides information about the disturbance ahead of the car and improves the transient behavior of the system when encountering changes in curvature. The effectiveness of the feedforward term depends on the quality of the curvature estimates. We discuss the curvature estimation process as part of the observer design in section 5.

4.3 Lane Change

Another task in addition to the controller keeping the vehicle in the lane, is the execution of a lane change maneuver. The lane change consists of a design of an open-loop trajectory and a controller for stabilizing the vehicle along the trajectory. In this case, both objectives are formulated at the look-ahead: *i.e.*, first we design a virtual trajectory for the offset at the look-ahead and then utilize the feedback controller introduced in the previous section to stabilize the vehicle around the desired trajectory. The proposed open-loop trajectory is based on commanded desired lateral acceleration. The desired trajectory for the offset at the look-ahead

$y_d(t)$ is expressed by fifth order polynomial in order to satisfy the constraints on lateral acceleration: \ddot{y}_d should be zero at the beginning and at the end of the maneuver. The desired steering angle for following an open-loop trajectory can be derived from the state equations and becomes:

$$\delta_{ref} = \frac{\ddot{y}_d}{\frac{c_f}{m} + \frac{Ll_f}{I_\phi}}. \quad (17)$$

The open-loop trajectory is designed for a particular speed, taking into account limits on lateral acceleration and jerk. The execution of the lane change maneuver has been carried out successfully in experiments at speeds around 40 mph. Since throughout the maneuver the lane markers are still being tracked by the vision system after the transition to the next lane, the lane following behavior can be robustly resumed.

5 Observer issues and design

In order to apply modern state space control techniques we require access to the states of the system. This is usually accomplished by constructing an observer. Our first step is to rewrite Equation 4 in the following form:

$$\dot{\mathbf{x}} = A(v_x)\mathbf{x} + B\delta_f \quad (18)$$

where $\mathbf{x} = [v_y, \dot{\psi}, y_L, \varepsilon_L, K_L]^T$ and

$$A(v_x) = \begin{bmatrix} -\frac{c_f+c_r}{mv_x} & -v_x + \frac{c_rl_r-c_f l_f}{mv_x} & 0 & 0 & 0 \\ \frac{-l_f c_f + l_r c_r}{I_\psi v_x} & \frac{-l_f^2 c_f + l_r^2 c_r}{I_\psi v_x} & 0 & 0 & 0 \\ -1 & -L & 0 & v_x & 0 \\ 0 & -1 & 0 & 0 & v_x \\ 0 & 0 & 0 & 0 & 0 \end{bmatrix} \text{ and } B = \begin{bmatrix} \frac{c_f}{m} \\ \frac{l_f c_f}{I_\psi} \\ 0 \\ 0 \\ 0 \end{bmatrix} \quad (19)$$

Note that the state vector \mathbf{x} has been augmented with the road curvature K_L since we are interested in estimating this parameter as well. This differential equation can be converted to discrete time in the usual manner by assuming that the control input, δ_f , is constant over the sampling interval T .

$$\mathbf{x}(k+1) = \Phi(v_x)\mathbf{x}(k) + \beta\mathbf{u}(k) \quad (20)$$

$$\Phi(v_x) = e^{A(v_x)T} \quad (21)$$

$$\beta = -\int_0^T e^{A(v_x)\tau} d\tau \quad (22)$$

Equation (20) allows us to predict how the state of the system will evolve between sampling intervals. Note that since the state evolution matrix $A(v_x)$ is parameterized by the vehicle speed, v_x , the discrete version, $\Phi(v_x)$ must be recalculated as the car accelerates and decelerates.

Measurements of the system state can be obtained from two sources: the vision system provides us with measurements of y_L and ε_L , while the on-board fiber optic gyro provides us with measurements of the yaw rate of the vehicle, $\dot{\psi}$. Our use of the yaw rate sensor measurements is analogous to the way in which

information from the proprioceptive system is used in animate vision. The measurements from the inertial sensor help us to distinguish changes in the image measurements that are due to the motion of the camera from changes that are due to the curvature of the road.

The measurement equations for our system can be written as follows:

$$\mathbf{y} = C\mathbf{x} \quad (23)$$

Where $\mathbf{y} = [\dot{\psi}, y_L, \varepsilon_L]^T$ and

$$C = \begin{bmatrix} 0 & 1 & 0 & 0 & 0 \\ 0 & 0 & 1 & 0 & 0 \\ 0 & 0 & 0 & 1 & 0 \end{bmatrix}. \quad (24)$$

The measurement vector \mathbf{y} can be used to update an estimate for the state of the system $\hat{\mathbf{x}}$ as shown in the following equation:

$$\hat{\mathbf{x}}^+(k) = \hat{\mathbf{x}}^-(k) + L(\mathbf{y}(k) - C\hat{\mathbf{x}}^-(k)) \quad (25)$$

where $\hat{\mathbf{x}}^-(k)$ and $\hat{\mathbf{x}}^+(k)$ denote the state estimate before and after the sensor update respectively.

The gain matrix L can be chosen in a number of ways [et al.94], depending on the assumptions one makes about the availability of noise statistics and the criterion one chooses to optimize. Regardless of the criterion chosen, the optimal choice for L will usually depend upon the transition matrix $\Phi(v_x)$ and hence on the vehicle speed v_x .

Since the measurements from the vision system are delayed by 57 milliseconds, the measurements of the other observer parameters, v_x , δ_f and $\dot{\psi}$ should also be delayed appropriately to ensure that the state update steps are carried out correctly. The state estimate can be projected forward to the current time by applying the state update equations.

6 Experimental Results

The controller has been tested both in simulation and in real experiments. In the simulation the full non-linear model of the vehicle has been used and the design has been tested for various road scenarios (see Figure 9). The maximum offset did not exceed 10 cm and the lateral acceleration was within passenger comfort standards. The initial experiments were carried out with the actual vehicle on the stretch of California highway, with speeds varying between 20-70 mph.

With the introduction of the lead-lag controller and an observer to filter noise from our measurements, we were able to take our experimental vehicle to speeds of 90 mph for extended periods of time without any degradation in passenger comfort. The lateral controller has been subsequently integrated into a system with a velocity controller, obstacle detection and avoidance system, and an intra-vehicle communication system.

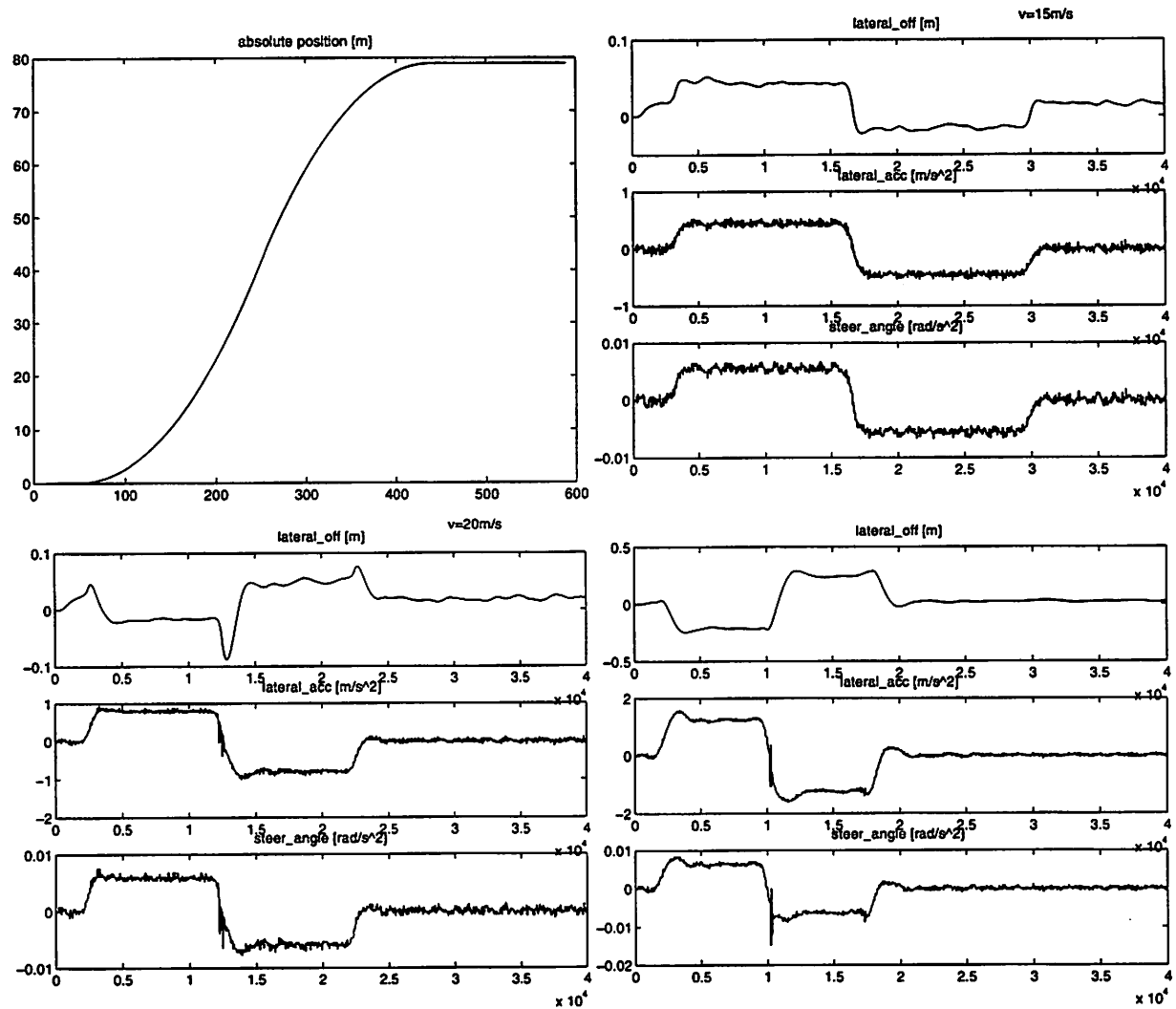


Figure 9: Tracking changes in curvature without intermediate straight line segments for various velocities. (a) reference path with straight line segment, followed by two curved segments with $K_{1ref} = 0.002 \text{ m}^{-1}$ and $K_{2ref} = -0.002 \text{ m}^{-1}$. (b) $v = 15 \text{ m/s}$ (c) $v = 20 \text{ m/s}$ (d) $v = 25 \text{ m/s}$. The look-ahead distance used in all experiments was $L = v 0.9 \text{ s}$.



Figure 10: Honda Accord used in experiments

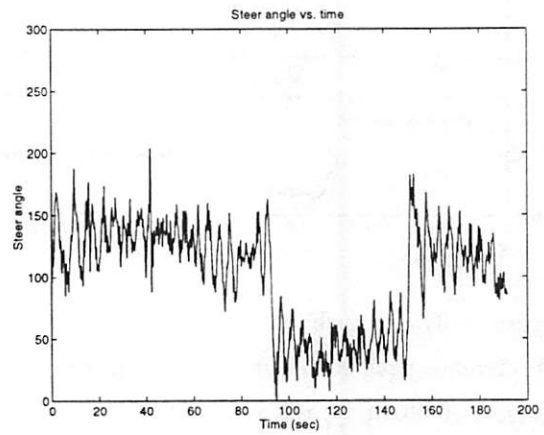
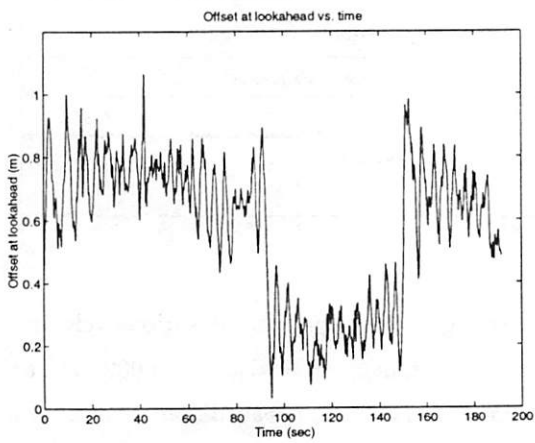


Figure 11: (a) The offset at the look-ahead y_L used for control purposes. (b) Commanded steering angle.

7 Conclusions

The main focus of this analysis was on the role of the look-ahead and the delay in the design of a steering controller.

The delay plays an important role in the system and should be taken into account explicitly in case of output feedback strategies, such as the ones we presented. We showed that sufficiently large look-ahead and appropriate choice of gain can compensate for the additional phase lag introduced by delay and vehicle dynamics at lower velocities. At higher velocities additional lead action was introduced in order to achieve desired phase margin. Since the criteria for passenger comfort put quite stringent limits on the bandwidth of the system an additional pole (lag) was necessary in order to keep the low bandwidth.

Formulating the regulation problem at smaller look-ahead distances improves the robustness of the system and increases the capability of tracking bigger changes in the curvature. The resulting controller has been tested both in simulation and experiments. Further experiments for different road scenarios and detailed performance evaluation of the experimental testbed are currently being performed.

Introducing a real-time observer process into the system not only reduces the noise inherent in the system's sensor measurements, but also provides an accurate estimate of the current vehicle state, circumventing the delay in the vision system and permitting the implementation of more advanced state-space based controllers.

References

- [Bla97] Robert. S. Blasi. A study of lateral controllers for the stereo drive project. Master's thesis, Department of Computer Science, University of California at Berkeley, 1997.
- [DM92] E. D. Dickmans and B. D. Mysliwetz. Recursive 3-D road and relative ego-state estimation. *IEEE Transactions on PAMI*, 14(2):199–213, February 1992.
- [ECR92] B. Espiau, F. Chaumette, and P. Rives. A new approach to visual servoing in robotics. *IEEE Transactions on Robotics and Automation*, 8(3):313 – 326, June 1992.
- [et al.94] Arthur Gelb *et al.* *Applied optimal estimation*. MIT Press, 1994.
- [FPEN94] G. F. Franklin, D. J. Powell, and A. Emani-Naeini. *Feedback control of dynamic systems, third edition*. Addison Wesley, 1994.
- [GTP96] J. Guldner, H.-S. Tan, and S. Patwarddhan. Analysis of automated steering control for highway vehicles with look-down lateral reference systems. *Vehicle System Dynamics (to appear)*, 1996.
- [Koř97] Jana Kořecká. Vision-based lateral control of vehicles:look-ahead and delay issues. Internal Memo, Department of EECS, University of California Berkeley, 1997.
- [Lan96] M. F. Land. The time it takes to process visual information when steering a vehicle. In *ARVO Poster B248, Investigative Ophthalmology*, 1996.

- [LL94] M. F. Land and D. N. Lee. Where we look when we steer? *Nature*, 369(30), June 1994.
- [MKS97] Yi Ma, Jana Košecká, and Shankar Sastry. Vision guided navigation for a nonholonomic mobile robot. In *submitted to CDC'98*, 1997.
- [ÖÜH95] Ü. Özgüner, K. A. Ünyelioglu, and C. Hatipoğlu. An analytical study of vehicle steering control. In *Proceedings of the 4th IEEE Conference on Control Applications*, pages 125 – 130, 1995.
- [Pen92] H. Peng. *Vehicle Lateral Control for Highway Automation*. PhD thesis, Department of Mechanical Engineering, University of California, Berkeley, 1992.
- [RH91] D. Raviv and M. Herman. A 'non-reconstruction' approach for road following. In Proceedings of the SPIE, editor, *Intelligent Robots and Computer Vision*, pages 2–12, 1991.
- [TMW96] Camillo J. Taylor, Jitendra Malik, and Joseph Weber. A real-time approach to stereopsis and lane-finding. In *Proceedings of the 1996 IEEE Intelligent Vehicles Symposium*, pages 207–213, Seikei University, Tokyo, Japan, September 19-20 1996.

Acknowledgment

This research has been supported by Honda R&D North America Inc., Honda R&D Company Limited, Japan, ITS MOU257 and MURI program DAAH04-96-1-0341.